



Design and Simulation of the Spiral Micromixer with Chaotic Advection

R. Prakash[†], M. Zunaid and Samsheer

Department of Mechanical Engineering, Delhi Technological University, Delhi, 110042, India

[†]Corresponding Author Email: ranjanprakash_2k18phdme16@dtu.ac.in

(Received July 30, 2022; accepted November 26, 2022)

ABSTRACT

In recent years, the microfluidics technique has screwed up rising attention and be in progress a fascinating topic. Species mixing is a compelling part of any microfluidic system that abides by the major challenge. In this research, a relative explication of mixing quality of microchannels of two cross-sections square and circular in spiral form is presented by numerical simulation. To perform the visitation, geometric parameters like axial length of microchannels and hydraulic diameter are taken equal for both cases. Computational Fluid Dynamics codes unriddle the Continuity equation, Navier-Stokes equation, and Convection-Diffusion equation. Explication of fluid flow and mixing have been gone through with an extensive limit of Reynolds numbers 1 to 125. The results explicate that the circular section spiral microchannel affords a higher mixing quality admixed to the square section spiral microchannel. Furthermore, in the circumstance of circular section spiral micromixer, mixing index esteem has attained 92% at $Re = 125$. For both section micromixer, the esteem of mixing index enhancement be contingent on Reynolds numbers. For both cases, pressure downfall has been computed for microchannels of similar lengths. The esteem of pressure downfall in square section spiral mixer is excess than circular section spiral mixer. The simulation outcomes exhibited that the circular section spiral micromixer is an effective design for microfluidic devices like Lab on a chip (LOC).

Keywords: Micromixing; Micromixer; Chaotic advection; Microfluidics; Simulation investigation.

NOMENCLATURE

c	mass fraction	V	velocity
D	diffusion coefficient	μ	fluid viscosity
M	mixing index	ρ	fluid density
p	pressure	σ	concentration variance
Re	Reynolds number		

1. INTRODUCTION

Microfluidics is the science that deals with the demeanor of fluids using micromixers and the technology of generating microminiaturized devices like Lab on a chip (LOC), giving various important advantages such as the use of the small volume of reagents compared to the large conventional mixer that results in huge saving of costly reagents per analysis, improved portability, low manufacturing cost, accurate measurement. Micromixer is the basic parts of microfluidics devices, which have a huge influence on biomedical diagnosis, medicine evolution, and chemical diligence for lab research like DNA Test, sample creation and study, cell separation, enzyme analysis, and protein folding. Also, a micromixer plays a vital role in the mixing of more than one sample for analysis. A nicely designed

mixer can decrease the analysis time and the footmark of a lab on a chip device. The mixer integrated with a microfluidic device like organ on chip will be used in the treatment of chronic diseases in the future.

Micromixers can be ranked as passive and active micromixers. Passive micromixers do not solicit outer impediments to raise mixing. Passive mixing relies on diffusion, split and recombination, and chaotic advection. Based on the order of mixed phases, passive mixing can be again ranked as serial lamination, parallel lamination, injection, droplet mixing, and chaotic advection. Active micromixers use outer impediments to speed up the mixing. Based on kinds of impediments, an active mixer can be ranked in temperature-induced, pressure-driven, electro-hydrodynamic, magneto-hydrodynamic,

electrokinetic, dielectrophoretic, acoustic concepts, electro-osmotic effect (arrangement of zeta-potential on walls), and piezo-electrically force. In a temperature-induced active mixer, fluids at varying temperatures are mixed in microchannel and a temperature gradient was created using two Peltier modules in the junction of a microchannel. Pressure-driven active micromixers are simple in design and construction. In this design, inject the fluid into the mixing channel alternately with the help of two micropumps generating a pulsatile flow. Making this arrangement rises the interfacial area outcoming in enhanced mixing quality. In electro-hydrodynamic (EHD), mixers use the movement of electrically charged fluids in an either Alternating Current (AC) electric field or a Direct Current (DC) electric field to unsettle the interface of mixing fluids that enhance diffusion species transport. In a magneto-hydrodynamic micromixer, an external magnetic field applied dc voltages on the electrodes can create Lorentz forces, that can fold and roll the fluids in mixing channel and make the fluids mix completely. An electrokinetic mixer utilizes electrokinetic flow to transport fluid. Electro-kinetic mixing is affected through a unique voltage source accompanied by channels dimensioned to take the hoped-for voltage segmentation. A novel dielectrophoretic micromixer is utilizing parallel microelectrodes to exploit the polymer particles and generate a vortex that can bustle the fluid to obtain mixing. Acoustically driven micromixer utilizes Surface Acoustic Waves (SAW). The acoustic wave is passed to the solid surface of mixer. The sound stream enhances the bustling effect which improves the mixing quality. In electro-osmotic micromixing, analysis of flow and mixing performance in a two-dimensional microchannel having nonuniform zeta potential on channel walls is accomplished. A piezo-electrical force-driven micromixer needs the erection of an interposed piezoelectric actuator and the wiring of a piezoelectric actuator for the external power supply.

Efficient and intense mixing is much important for these exercises. The mixing process is a difficult process for low Reynolds number flow inside the micromixer. Simple T-junction and Y-junction micromixing mainly depend on molecular diffusion, which is much slower. So it is essential to utilize especially drafted micromixers to speed up the mixing process.

In this context, [Azmi *et al.* \(2021\)](#) deciphered the effect of the hybrid composition ratio for wire coil flow. [Balasubramaniam *et al.* \(2017\)](#) reported the enhancement of mixing quality in spiral micromixers of different cross-sections (rectangular, square, semi-circular, trapezoidal) and hydraulic diameters. [Chen and Chen \(2019\)](#) collated mixing index of circular micromixer and topology-based passive micromixers. [Cao *et al.* \(2021\)](#) developed a model to describe liquid-gas flow in an inclined and horizontal pipe. [Dong *et al.* \(2020\)](#) visited the impression of DC and AC electric fields on the mixing index in a microchannel. [Farahinia *et al.* \(2021\)](#) presented a simulation analysis of electro-osmotic flow in heterogeneous micromixers and also examined micromixer performance with combined

effects of electro-osmotic and pressure-driven flows. [Farahinia *et al.* \(2020a\)](#) contributed a comprehensive review of various separation systems of Circulating Tumor Cells engendering from the primary tumor or cancer tissue. Nowadays some researchers are using microfluidic devices for Circulating Tumor Cells separation from the blood cells. Lab on a chip (LOC) and then Lab on a CD (LOCD) are the recent trends. [Farahinia *et al.* \(2020b\)](#) presented two cross-sections of T-Junction microchannel namely circular cross-section and rectangular cross-section and studied the effects of input angles on mixing efficiency. [Farahinia and Zhang \(2019\)](#) studied the optimal design of a passive T micromixer having assigned patterns of blockades and grooves with various geometries. [Ghazimirsaeed *et al.* \(2021\)](#) explored the impact of rectangular cross-section serpentine microchannel with three aspect ratios and another three cross-section geometry like circular, triangular, and trapezoidal on mixing performance. [Hasanah *et al.* \(2022\)](#) designed micromixers having Koch Fractal Obstacle and studied the effect of two different inlet conditions and resistance angles. [Hossain *et al.* \(2009\)](#) formulated the problem of three different microchannels and analyzed the pressure downfall and mixing quality of these microchannels. [Jiang *et al.* \(2022\)](#) explicated the various shapes of cross-sections like triangular and elliptical and inserted different obstacles like hexagonal, triangular, and cylindrical in variable radius spiral microchannel. [Kockmann *et al.* \(2003\)](#) analyzed liquid mixing in simple static mixers having different cross-sections like rectangular, square, and trapezoidal.

[Li *et al.* \(2012\)](#) explicated the impression of a small width outlet and turning angle in a zigzag microchannel. [Liu *et al.* \(2022\)](#) proposed a microchannel transacted by two piezoelectric micropumps having multi-stage mixing. This micromixer is combination of novel texture and piezoelectric drive technique to create a novel mixing technique, which provides excellent mixing quality. [Liu *et al.* \(2018\)](#) designed and created a self-circulation microchannel having high-frequency vibration rely on the piezoelectric drive technique. Piezoelectric lead-zirconate-titanate (PZT) micropumps integrated with microchannel are used to generate self-circulation reflux in the mixing chamber and give a better working performance with compelling frequency of 80-120 Hz. [Mondal *et al.* \(2021\)](#) created a serpentine microchannel in a square waveform by the use of the WEDM process. [Nezhad *et al.* \(2018\)](#) offer baffles in three different forms in the microchannel and observed these baffles effects on the mixing index. [Nouri *et al.* \(2017\)](#) explicated the influence of ferrofluid and water mixture on mixing index by use of a magnetic field. [Prakash *et al.* \(2021\)](#) inspected the impression of a T-bend mixing channel at various radii. [Pang *et al.* \(2020\)](#) presented a T-form microfluidic device with a neck at the junction and evaluate droplet volume under several flow rates. [Quiyoom *et al.* \(2017\)](#) deciphered the free surface effect on liquid-phase mixing in shallow vessels. [Redapangu *et al.* \(2021\)](#) analyzed the effect of changing density and viscosity of two immiscible liquids in a 3-D inclined

microchannel. [Ruijin *et al.* \(2017\)](#) likened mixing quality of three mixers Baker, Smale, and Helical. [Rouhi *et al.* \(2021\)](#) studied the cross-sections effects on mixing quality of spiral microchannel in Reynolds number limit from 0.001 to 50. [Santana *et al.* \(2019\)](#) examined the impose of circular form obstructions and triangular form baffles in the micromixer with ethanol and oil mixture. [Seo and Kim \(2012\)](#) designed a passive and active combination micromixer and collated the mixing index esteem of passive micromixer with various obstacles and active micromixer under an external electric field. [Saleel *et al.* \(2020\)](#) analyzed the impose of changing the height of a rectangular block in a micromixer in the concern of Electro-osmotic flow. [Shinde *et al.* \(2021\)](#) examined mixing quality of SARM having U-form, V-form, and square C-form pillars located in a microchannel. [Shimizu and Uetsuji \(2022\)](#) proposed two drive modes single and double Metal-capped bimorph actuator (MC-BMP) and compared the mixing index and flow rate with conventional BMP (Bimorph). [Tokas *et al.* \(2021\)](#) monitored the effect of working fluid as blood in a T-helical microchannel. [Tony *et al.* \(2021\)](#) generalized the concept of Integrated Microfluidic Circuit (IMC) to the conception designated soft microfluidic system (SMS). It includes a soft robotic microfluidic system, which can show robotic behaviors, like movement, control, sensing, and actuation. [Umadevi *et al.* \(2021\)](#) introduced a study about blood and copper nanoparticles in a water mixture in an inclined artery under an external magnetic field. [Vatankhah and Shamloo \(2018\)](#) calibrated the mixing quality of helical-type microchannels.

[Wu *et al.* \(2021\)](#) anatomized the effect of swirl motion in a jet mixer for liquid mixing. [Xia *et al.* \(2016\)](#) explored the impose of gaps and baffles at different positions in a planar micromixer. [Xu *et al.* \(2011\)](#) read out the fluid motion and pressure drop in a staggered oriented ridges micromixer. [Yang *et al.* \(2022\)](#) reviewed Microfluidic Point of Care (POC) instruments and their uses. Microfluidic POC tools can hurriedly retrace diseases at a minimum cost. This technique is used to find out diseases in immature regions to decrease the impacts of disease and enhance the potency of life in these regions. [Zhang *et al.* \(2019\)](#) created fractal baffles in a T microchannel and likened the mixing quality of primary and secondary fractals.

Contemplating the literature exploration, in this paper square section spiral micromixer and circular section spiral micromixer are explicated and similitude the mixing index of square section spiral micromixer and circular section spiral micromixer. Then the impose of Reynolds number is examined for both cross-sections. The outcomes report that a circular section spiral mixer is more verseed than a square section spiral mixer. The advantages of micromixer proposed in this study are that better mixing quality than simple T junction, Y junction, and serpentine micromixers. Also presented circular section spiral micromixer is a better configuration than a square section spiral micromixer for microfluidic devices namely Lab on a chip (LOC).

2. DELINEATION OF THE MICROMIXER

Square section spiral micromixer and circular section spiral micromixer are explicated in Fig. 1. Two configurations are square and circular with two inlets in which water is flowing from one inlet and the water-soluble dye is flowing through the second inlet. For the relative study, hydraulic diameter of the mixing channel and inlets channel of both configurations was elected equal. Geometry descriptions are provided in Table 1.

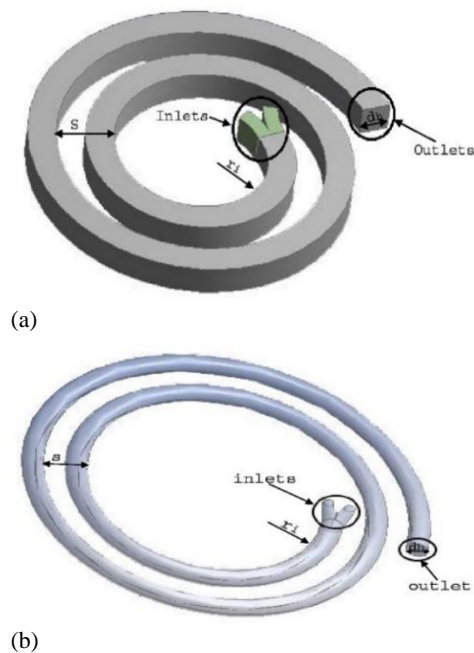


Fig.1 Microchannels of two cross-sections (a) square (b) circular.

Table 1 Configuration mensuration of square section spiral micromixer and circular section spiral micromixer.

Type	Square section spiral micromixer	Circular section spiral micromixer
Hydraulic diameter of mixing channel	0.2 mm	0.2 mm
Hydraulic diameter of inlets channel	0.133 mm	0.133 mm
The distance between two successive turnings, s	0.4 mm	0.4 mm
initial microchannel radius, r_i	1 mm	1 mm
Number of turns, N	2	2
The total spiral length	15 mm	15 mm

In this paper, the spiral curvature of varied cross-sections is introduced so in this case, secondary flow creates, which tends to interact between centrifugal and inertia forces. The centrifugal forces poke the liquid from the centre of the microchannel to an outer wall, where the liquid has less velocity. At the outside wall, a double vortex creates by squeezing the liquids and parenting the liquids move in downward and upward directions. On the other side, the viscid wall friction moistens both vortexes by working as opposed to centrifugal force, which relies on average liquid velocity and curvature radius. As stated by Dean, the flow dominations and creation of vortices in a laminar region with a small Reynolds number in curvature rely on the dimensionless number named Dean Number. It is interpreted as:

$$De = Re \sqrt{\frac{D_h}{2R}} \quad (1)$$

Where R is the microchannel curvature radius, Re is the Reynolds number, and D_h is the hydraulic diameter. If the value of De is less than one, the mixing of two fluids is primely obtained by diffusion. If Dean number is greater than ten, the first double vortex creates and improves micro mixing.

Reynolds number is demonstrated as the proportion of inertia force to the viscous force. Mathematically, it is expressed as:

$$Re = \frac{\rho v D_h}{\mu} \quad (2)$$

Where ρ is density of fluid, v is velocity of fluid, and μ is absolute viscosity of fluid.

The hydraulic diameter D_h is evaluated by equation (3), as exhibited below:

$$D_h = \frac{4A}{P} \quad (3)$$

Where A is a cross-section area and P is the perimeter of the cross-section of the mixing channel.

3. SIMULATION ACCESSORY

To anatomize the mixing process and flow in the microchannels, the Computational Fluid Dynamics (CFD) tool Ansys Fluent has been utilized. By application of finite volume technique, Fluent code elucidates the momentum and continuity equations. For computing the fluid motion, Fluent-solver will figure out the adequate mean values of the characteristic of every control mass in the stream zone. These mean esteems rely on magnitudes of constituent characteristics and the rates of every constituent which is extant in the control mass. In the concern of two or more fluids, the retention is rendered that fluids are mingled at the molecular scale and characteristics of fluids rely on similitudes of components. The embracement is as well created that mass fraction pullulates through diffusion and convection. The differential movement of particular constituents in the species mixture is numerated by genitive mass flux. This mass flux is imitated by the

impression of concentration gradients, pressure gradients, etc. The governing equations are illustrated in [Shinde *et al.* \(2021\)](#) and indicated in equations (4) to (6) as:

$$\nabla v = 0 \quad (4)$$

$$\rho \left[\frac{\partial v}{\partial t} + (v \cdot \nabla) v \right] = -\nabla p + \mu \nabla^2 v \quad (5)$$

$$\frac{\partial c}{\partial t} = D \nabla^2 c - v \cdot \nabla c \quad (6)$$

Where, viscosity μ , density ρ , diffusion coefficient D, velocity v, pressure p, mass fraction c, and Del operator ∇ .

$$\nabla = \frac{\partial}{\partial x} \hat{i} + \frac{\partial}{\partial y} \hat{j} + \frac{\partial}{\partial z} \hat{k}$$

A scant quantity of dye diluted in water and pure water is utilized as two operative fluids for mixing. Since the dye is diluted in water in a very small quantity, so characteristics of both water and water dye will be approx. same. The characteristics of water and water-dye have been selected at 20°C and values are taken as, the diffusivity for mixture (D) is $10^{-10} \text{ m}^2/\text{s}$, the viscosity of water (μ) is 0.001 Ns/m^2 , the density of water (ρ) is 1000 kg/m^3 . The same inlet velocity and zero gauge outlet pressure are elaborated as the boundary conditions. Water and water with dye are allocated to inlet1 and inlet2 with mass fraction zero and one respectively. The no-slip circumstances were enforced on the parapets. The results are recognized to have reached convergence when the residual esteem is maximally 10^{-8} .

The mixing quality is admeasured by numerating the concentration variance of composition in a microchannel. To estimate intensity of tincture in a microchannel, a variance of concentration of composition at cross-section is determined as presented in [Hossain *et al.* \(2009\)](#):

$$\sigma = \sqrt{\frac{1}{N} \sum (C_i - C_m)^2} \quad (7)$$

In above elucidation, N is total sampling point at the cross-section, C_i is the concentration at sampling point, i, and C_m is mean of the concentrations. In this affair, N on every plane was 500 to maintain high accuracy. To examine the mixing efficiency of microchannel, mixing index is determined as:

$$M = 1 - \sqrt{\frac{\sigma^2}{\sigma_{max}^2}} \quad (8)$$

Where σ is standard deviation value at cross-section and σ_{max} is maximum standard deviation. A supreme mixing index denotes a supreme mixing quality. For separate streams mixing index esteem is zero and for fully mixed streams mixing index esteem is one.

4. RESULTS AND DISCUSSION

The mixing index is enhanced by geometry transformation. For this goal, two microchannels of

varied cross-sections square and circular have been simulated and admixed the mixing index results of both channels square and circular cross-sections. As well scrutinize the impose of Reynolds numbers on pressure drop and mixing index.

4.1 Mesh Generation and Grid Sensitivity Analysis

Mesh generation in a square cross-section and circular cross-section spiral micromixer with tetrahedral type mesh is presented in Fig. 2(a) and Fig. 2(b). To search out the best grid elements, this is essential to calibrate that the rectification is grid-independent. Five diverse mesh systems 1.9 million, 3.9 million, 5.1 million, 5.5 million, and 6.3 million were tested for both microchannels. Numerated mixing index at the outlet is revealed in Fig. 2(c), as can be looked over in this diagram, the numerated mixing index reduces with increasing the number of grid elements. This is due to less molecular diffusion in the case of increasing the number of grid cells. However, mixing index numerated with 5.5 million and 6.3 million give no more significance difference. So from grid independency, 5.5 million was elected as the best grid for all simulations.

4.2 Validation of computational work

The existing simulation work is admixed with the numerical outgrowths of [Vatankhah and Shamloo \(2018\)](#) for the same Reynolds number and microchannel length as explicated in Fig. 3. The mixing index versus Reynolds number graph has been plotted for the outlet of a microchannel. The outgrowths exhibit compatible consent between the existing workout and [Vatankhah and Shamloo \(2018\)](#) work with a maximum percentage error of 5.7.

4.3 Sequel of modified geometry

To interpret the simulation results, mixing index of simulations is compared at the outlet of square and circular cross-section spiral micromixer. The dispersions of concentration of microchannel of square cross-section and circular cross-section at Reynolds number 125 are explicated in Fig. 4. This concentration contour explicates that mixing quality in circular cross-section microchannel is of high quality than square cross-section microchannel. To illustrate the influence of circular cross-section on mixing quality, the power of vortices created inside a cross-section can be scaled by swirling strength, which is defined as the proportion of the tangential velocity of the fluid to the main velocity along a plane. Because of creation of vortices inside micromixers, velocity created at the centric region isolating the two vortices is much improved, outcoming in supreme swirling strength in a spiral or curved microchannels in similitude to a straight microchannel. It is got that circular cross-section microchannel obtain supreme mixing quality than square cross-section microchannel because of their enhanced swirling strength. Also, the mass fraction variations in circular cross-section microchannel at

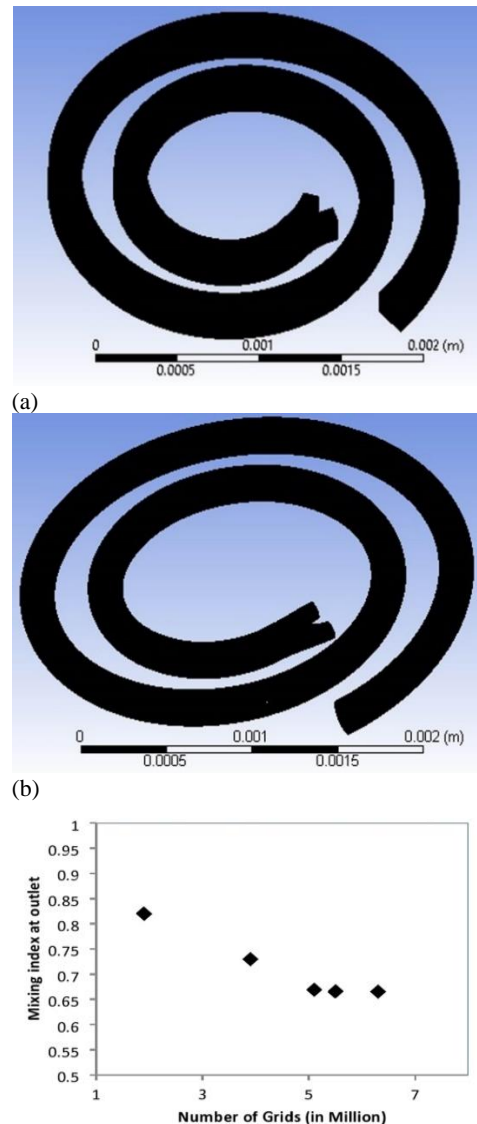


Fig. 2: (a) Tetrahedral mesh of square cross-section spiral micromixer (b) Tetrahedral mesh of circular cross-section spiral micromixer (c) Numerated mixing quality at outlet and number of the grid element.

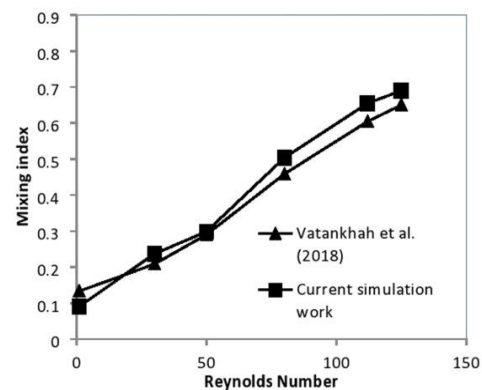
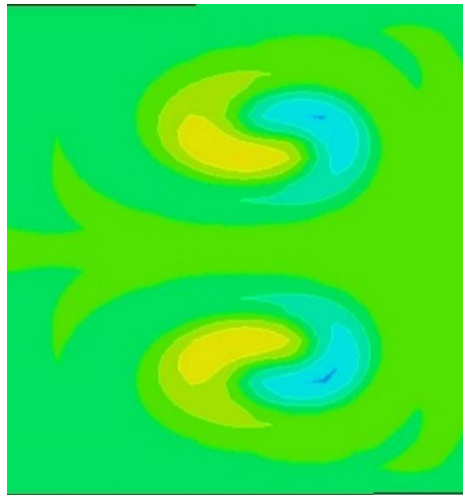
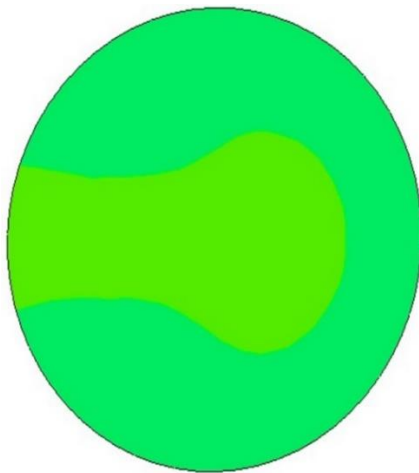


Fig. 3 Collation of mixing index of current square section microchannel and previously published data.



(a)



(b)

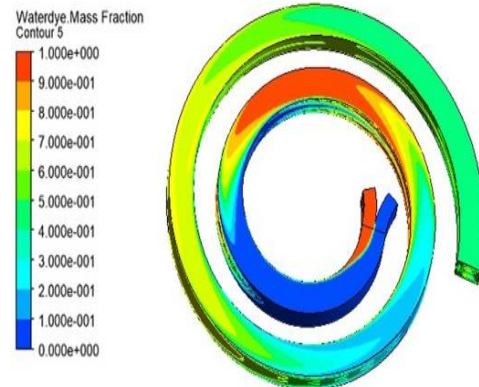
Fig. 4 Concentration contours of microchannel (a) square cross-section (b) circular cross-section at $Re = 125$.

an outlet achieves near to optimal mixing mass fraction esteem i.e 0.5 mol/m^3 but in the case of square cross-section microchannel, mass fraction variations at an outlet are in a wide range. So we require extra microchannel length and extra time to get the same outcomes as circular cross-section microchannel. The worth of mixing index at an outlet for a circular cross-section mixing channel is ($M = 92.95$) while for a square cross-section mixing channel is ($M = 84.20$).

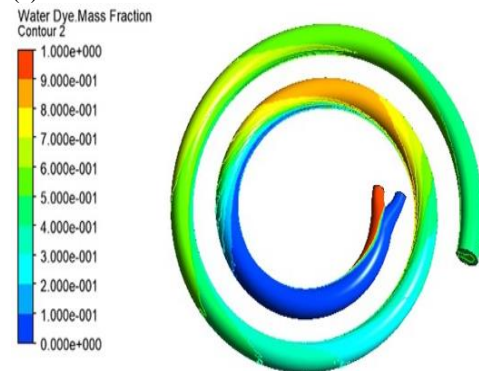
Figure 5 explicates a mass fraction contour along the helical length in square cross-section and circular cross-section microchannel. The figure displays that at this high Reynolds number, mixing rises consistently from the junction point to the outlet. The red color reports one fluid (water) and the blue color reports another fluid (dye diluted in water). When mixing has occurred, delineates green color.

The mixing is more influenced through secondary flow generated due to centrifugal force in the case of circular cross-section microchannel as compared to square cross-section microchannel. So chaotic advection is more effective in circular cross-section spiral micromixer as compared to square cross-

section spiral micromixer, which prominently improves mixing. This incidence can be seen by streamlines rely on mass fraction. The streamlines rooted on mass fraction ubiquitously the helical length in square and circular cross-section microchannel are explicated in Fig. 6. These streamlines illustrate the deviation in mixing quality pattern executed amid square and circular section microchannel. A more advanced perusal was executed to scrutinize the alteration of mixing quality of square and circular cross-section microchannels at different part length along the direction of flow. At Reynolds number = 125, the mixing quality rapidly increases from 14.6 % at a distance of 1mm to 77.2 % at a distance of 10mm in the concern of square cross-section spiral micromixer and 22.6% at a distance of 1mm to 90.3 % at a distance of 10mm in concern of circular cross-section spiral micromixer intimating the benefit of implementing circular section microchannel for high Reynolds number. The concentration contours at four positions starting from the junction point for square cross-section microchannel and circular cross-section microchannel are explicated in Fig. 7 and Fig. 8 delineates the velocity vector plots at outlet of microchannel square and circular cross-section. At Reynolds number = 125, the flow sample is nearly identical in both channels, and velocity vectors are curvilinear to a microchannel wall throughout the cross-section.



(a)



(b)

Fig. 5 Mass fraction contour along helical length for (a) square cross-section microchannel (b) circular cross-section microchannel at $Re = 125$.

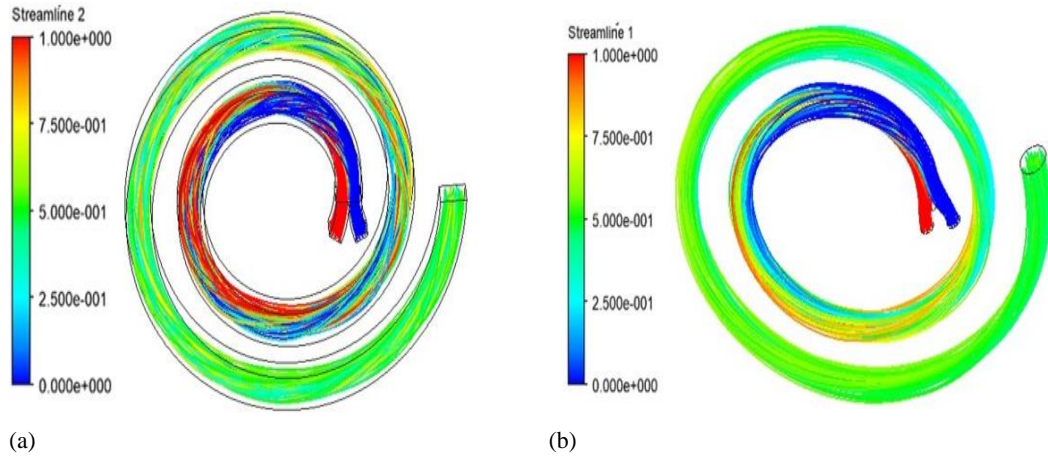


Fig. 6 Streamlines rooted on species concentration for microchannel of (a) square cross-section (b) circular cross-section at $Re = 125$.

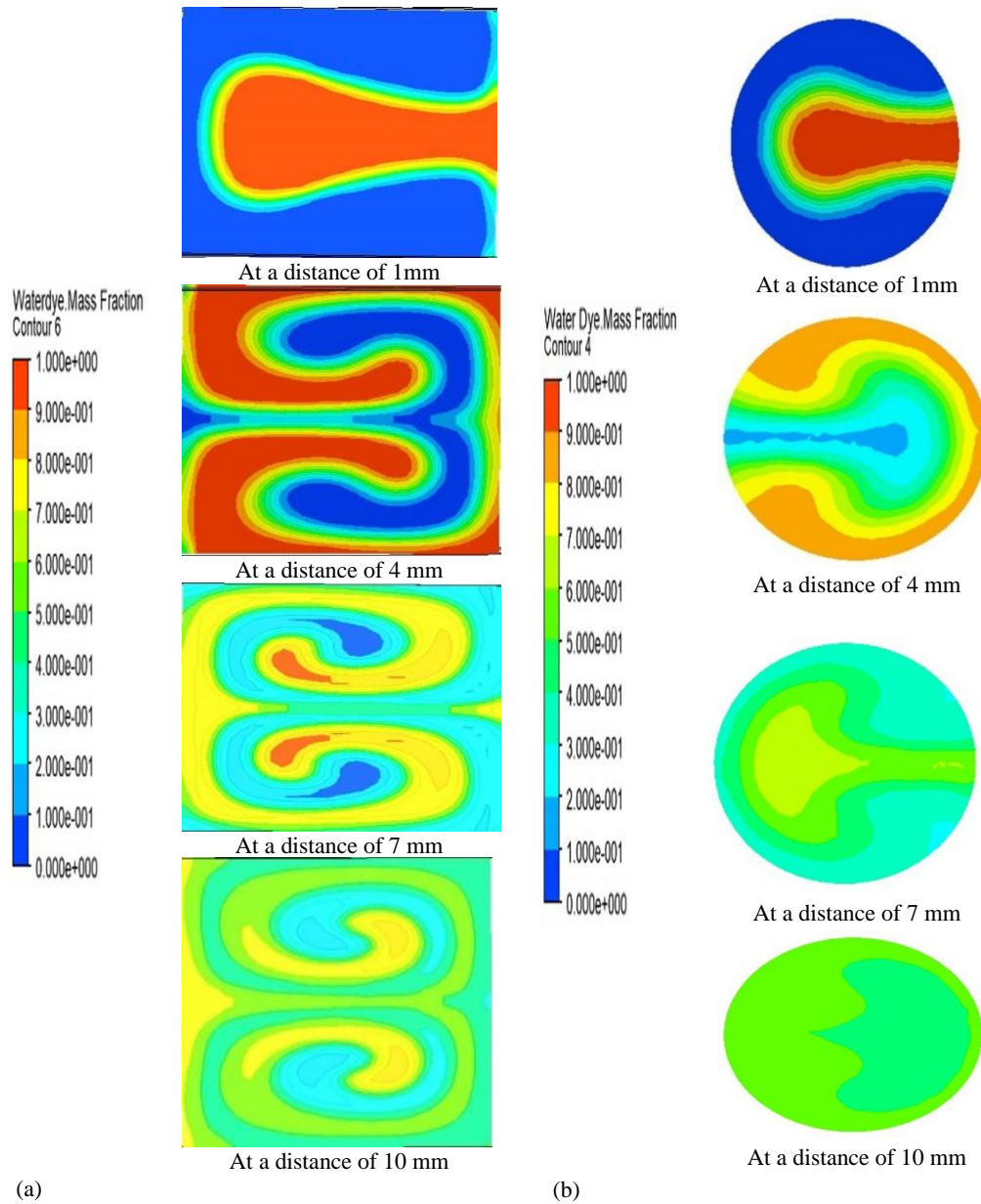
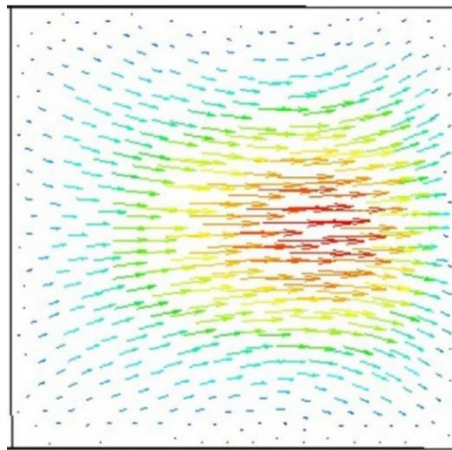
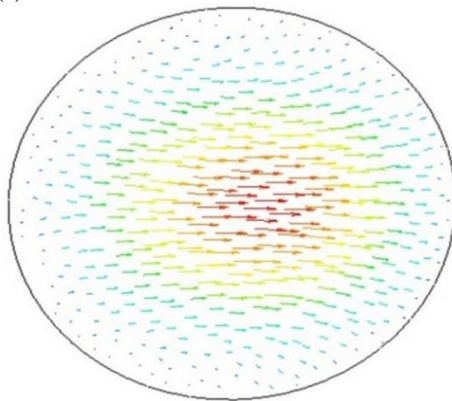


Fig. 7 Contour of species concentration at four different locations starting from junction point for microchannel of (a) square cross-section (b) circular cross-section at $Re = 125$.



(a)



(b)

Fig. 8 Velocity vectors plot for microchannel of (a) square cross-section (b) circular cross-section at $Re = 125$.

4.4 Imposingness of Reynolds Number

The Reynolds number imposingness on the mixing quality in both microchannel square and circular cross-sections was deciphered. The simulation process was performed with Reynolds numbers (1, 30, 50, 80, 112, and 125) for square cross-section microchannel and circular cross-section microchannel having a fixed length.

Figure 9 explicates the plots between mixing index and Reynolds numbers in which circular cross-section microchannel have better mixing quality.

The interpretation of mixing continual solicits the perusal of pressure drop amid inlet and outlet of mixing channel and this happens more valuable in concern of passive mixers because the pressure falls instants an opinion of the power which will be needed to pump the fluids from inlet to outlet. So, it is necessary to examine the pressure drop in a microchannel. The mixing process uses energy inputs in terms of pressure drops. Figure 10 delineates alteration of pressure downfall for the two configurations at multifarious Reynolds numbers. For both concerns, the pressure falls have been worked out for microchannels with the same streamwise lengths. The pressure falls rise suddenly with the Reynolds number for both the microchannel. The circular cross-section

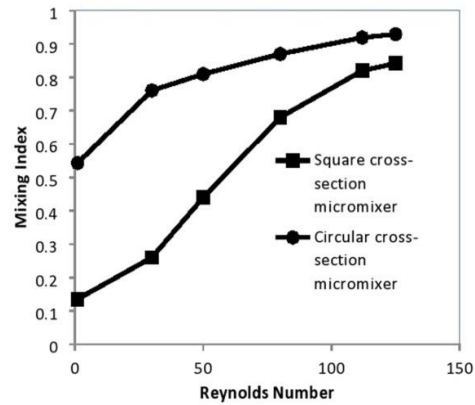


Fig. 9 Mixing index values for square and circular cross-section microchannel at various Reynolds numbers.

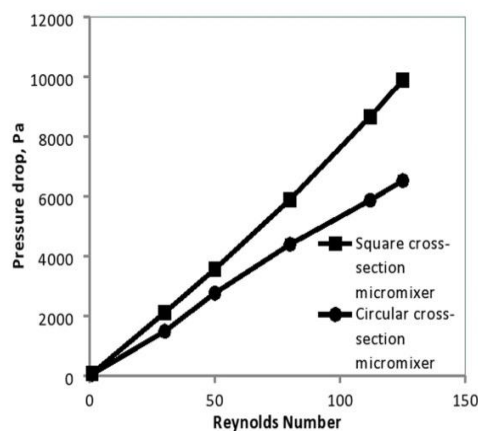


Fig. 10 Alteration of the pressure fall with Reynolds number for both geometry.

microchannel explicates lesser pressure drop than the square cross-section microchannel because there are no sharp edges in the circular cross-section microchannel. Figure 11 explicates dispensations of mixing index along streamwise length at Reynolds number 125. The mixing rises well-orderly along microchannel length as delineated in this diagram.

5. CONCLUSIONS

In this work, the numerical perusal of mixing in square and circular cross-section microchannels has been exploited. Dye diluted in water solution and pure water have been elected as working fluids for mixing. Navier-Stokes in three-dimensional explores flow field and mixing for Reynolds numbers 1 to 125. It was educed that circular cross-section microchannel explicates a superior mixing quality than square cross-section microchannel. In both microchannels, the pressure downfalls suddenly rise with the Reynolds number. The circular cross-section microchannel shows smaller pressure drops than the square cross-section microchannel. The tenor of this exploration is to get two objectives which are

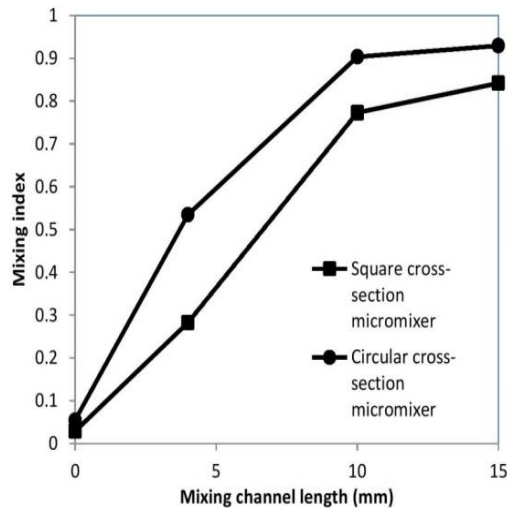


Fig. 11 Dispensations of mixing index along streamwise length at $Re = 125$.

supreme mixing quality and small pressure drops in the microchannels. The circular cross-section mixing channel has fulfilled both criteria, so this cross-section is better for fluids mixing. In actual practice, the operation of a Lab on a chip system is not affected through pressure drop. The design plays an important role, so this circular cross-section mixing channel has a good potential for use in lab on a chip device. To design the next generation micromixer, the phenomenon of cavitation inside the micromixer will be considered in the future. Also, future studies will be focused on computational analysis of mixing of different fluids like blood mixture, water-ethanol mixture, water-ink mixture, etc because mixing quality depends on the diffusion coefficient of fluids mixture.

ACKNOWLEDGEMENTS

This work was encouraged by Delhi Technological University, Delhi.

CONFLICT OF INTEREST

The authors reveal that there is no conflict of interest regarding the publication of this paper.

REFERENCES

Azmi, W. H., K. A. Hamid, A. I. Ramadhan and A. I. M. Shaiful (2021). Thermal hydraulic performance for hybrid composition ratio of TiO_2 - SiO_2 nanofluids in a tube with wire coil inserts. *Case Studies in Thermal Engineering* 25, 100899.

Balasubramaniam, L., R. Arayanarakool, S. D. Marshall, B. Li, P. S. Lee and P. C. Y. Chen (2017). Impact of cross-sectional geometry on mixing performance of spiral microfluidic channels characterized by swirling strength of Dean-vortices. *Journal of Micromechanics and Microengineering* 27, 095016.

Cao, X., K. Yang, T. Li, N. Xiong, W. Yang and J. Bian (2021). Numerical simulation of hydrate particle behaviors in gas-liquid flow for horizontal and inclined pipeline. *Case Studies in Thermal Engineering* 27, 101294.

Chen, Y. and X. Chen (2019). An improved design for passive micromixer based on topology optimization method. *Chemical Physics Letters* 734, 136706.

Dong, S., P. F. Geng, D. Dong and C. X. Li (2020). Mixing enhancement of electroosmotic flow in microchannels under DC and AC electric field. *Journal of Applied Fluid Mechanics* 13(1), 79-88.

Farahinia, A., J. Jamaati, H. Niazmand and W. Zhang (2021). The effect of heterogeneous surface charges on mixing in a combined electroosmotic/pressure-driven micromixer. *Journal of the Brazilian Society of Mechanical Sciences and Engineering* 43, 497.

Farahinia, A., W. J. Zhang and I. Badea (2020a). Circulating Tumor Cell Separation of Blood Cells and Sorting in Novel Microfluidic Approaches: a review. *Journal of Science: Advanced Materials and Devices* doi: 10.20944/preprints202010.0622.v1.

Farahinia, A. and W. J. Zhang (2020b). Numerical analysis of a microfluidic mixer and the effects of different cross-sections and various input angles on its mixing performance. *Journal of the Brazilian Society of Mechanical Sciences and Engineering* 42, 190.

Farahinia, A. and W. J. Zhang (2019). Numerical investigation into the mixing performance of micro T-mixers with different patterns of obstacles. *Journal of the Brazilian Society of Mechanical Sciences and Engineering* 41, 491.

Ghazimirsaeed, E., M. Madadelahi, M. Dizani and A. Shamloo (2021). Secondary flows, mixing, and chemical reaction analysis of droplet based flow inside serpentine microchannels with different cross-sections. *Langmuir* 37(17), 5118-5130.

Hasanah, L., D. F. Nurvadila, R. E. Pawinanto, B. Mulyanti, C. Wulandari, A. Aminudin and J. Yunas (2022). A passive micromixer with Koch Snowflakes Fractal obstacle in microchannel. *Journal of Applied Fluid Mechanics* 15(5), 1333-1344.

Hossain, S., M. A. Ansari and K. Y. Kim (2009). Evaluation of the mixing performance of three passive micromixers. *Chemical Engineering Journal* 150, 492-501.

Jiang, Y., B. Zhang, Y. Tian, Y. Zhang and Y. Chen (2022). Analysis of different shapes of cross-sections and obstacles in variable-radius spiral micromixers on mixing efficiency. *Chemical Engineering and Processing Process Intensification* 171, 108756.

- Kockmann, N., M. Engler, C. Föll and P. Woias (2003). Liquid mixing in static micromixers with various cross-sections. In *1st International Conference on Microchannels and Minichannels* 911-918.
- Li, Y., D. Zhang, X. Feng, Y. Xu and B. F. Liu (2012). A microsecond microfluidic mixer for characterizing fast biochemical reactions. *Talanta* 88, 175-180.
- Liu, G., M. Wang, P. Li, X. Sun, L. Dong and P. Li (2022). A micromixer driven by two valveless piezoelectric pumps with multistage mixing characteristics. *Sensors and Actuators: A. Physical* 333, 113225.
- Liu, G., X. Ma, C. Wang, X. Sun and C. Tang (2018). Piezoelectric driven self-circulation micromixer with high frequency vibration. *Journal of Micromechanics and Microengineering* 28, 085010.
- Mondal, B., S. Pati and P. K. Patowari (2021). Serpentine square wave microchannel fabrication with WEDM and soft lithography. *Materials Today: Proceedings* 46, 8513-8518.
- Nezhad, J. R. and S. A. Mirbozorgi (2018). An immersed boundary-lattice Boltzmann method to simulate chaotic micromixers with baffles. *Computers and Fluids* 167, 206-214.
- Nouri, D., A. Z. Hesri and M. P. Fard (2017). Rapid mixing in micromixers using magnetic field. *Sensors and Actuators A* 255, 79-86.
- Pang, Y., Q. Zhou, X. Wang, Y. Lei, Y. Ren, M. Li, J. Wang and Z. Liu (2020). Droplets generation under different flow rates in T-junction microchannel with a neck. *AIChE Journal* 66(10), 16290.
- Prakash, R., M. Zunaid and Samsher (2021). Simulation analysis of mixing quality in T-junction micromixer with bend mixing channel. *Materials Today: Proceedings* 47, 3833-3838.
- Quiyoom, A., V. V. Buwa and S. K. Ajmani (2017). Role of free surface on gas-induced liquid mixing in a shallow vessel. *AIChE Journal* 63(8), 3582-3598.
- Redapangu, P. R., T. G. Kidan and K. Berhane (2021). Mixing and interpenetration in a three dimensional Buoyancy-Driven flow of two immiscible liquids: A GPU based LBM Approach. *Journal of Applied Fluid Mechanics* 14(2), 601-613.
- Rouhi, O., S. R. Bazaz, H. Niazmand, F. Mirakhorli, S. M. hafi, H. A. Amiri, M. Miansari and M. E. Warkiani (2021). Numerical and experimental study of cross-sectional effects on the mixing performance of the spiral microfluidics. *Micromachines* 12, 1470.
- Ruijin, W., L. Beiqi, S. Dongdong and Z. Zefei (2017). Investigation on the splitting-merging passive micromixer based on Baker's transformation. *Sensors and Actuator B* 249, 395-404.
- Saleel, C. A., A. Algahtani, I. A. Badruddin, T. M. Yunus Khan, S. Kamangar and M. A. H. Abdelmohimen (2020). Pressure-Driven Electro-Osmotic Flow and Mass Transport in Constricted Mixing Micro-channels. *Journal of Applied Fluid Mechanics* 13(2), 429-441.
- Santana, H. S., J. L. Silva Jr and O. P. Taranto (2019). Optimization of micromixer with triangular baffles for chemical process in millidevices. *Sensors and Actuators B: Chemical* 281, 191-203.
- Seo, H. S. and Y. J. Kim (2012). A study on the mixing characteristics in a hybrid type microchannel with various obstacle configurations. *Materials Research Bulletin* 47, 2948-2951.
- Shimizu, H. and Y. Uetsuji (2022). Fluid-structure and electric coupled analysis of a valveless microfluidic system using metal-capped piezoelectric actuator. *Sensors and Actuators A: Physical* 333, 113232.
- Shinde, A. B., A. V. Patil and V. B. Patil (2021). Enhance the mixing performance of water and ethanol at micro level using geometrical modifications. *Materials Today: Proceedings* 46, 460-470.
- Tokas, S., M. Zunaid and M. A. Ansari (2021). Non-Newtonian fluid mixing in a Three Dimensional spiral passive micromixer. *Materials Today: Proceedings* 47, 3947-3952.
- Tony, A., A. Rasouli, A. Farahinia, G. Wells, H. Zhang, S. Achenbach, S. M. Yang, W. Sun and W. Zhang (2021). Toward a Soft Microfluidic System: Concept and Preliminary Developments. In *27th International Conference on Mechatronics and Machine Vision in Practice*, 755-759.
- Umadevi, C., M. Dhange, B. Haritha and T. Sudha (2021). Flow of blood mixed with copper nanoparticles in an inclined overlapping stenosed artery with magnetic field. *Case Studies in Thermal Engineering* 25, 100947.
- Vatankhah, P. and A. Shamloo (2018). Parametric study on mixing process in an in-plane spiral micromixer utilizing chaotic advection. *Analytica Chimica Acta* 1022, 96-105.
- Wu, B., C. Li, M. Zhand and P. Luo (2021). Liquid mixing intensification by adding swirling flow in the transverse jet mixer. *AIChE Journal* 67(8), 17276.
- Xia, G. D., Y. F. Li, J. Wang and Y. L. Zhai (2016). Numerical and experimental analyses of planar micromixer with gaps and baffles based on field synergy principle. *International Communications in Heat and Mass Transfer* 71, 188-196.

Xu, Z., C. Li, D. Vadillo, X. Ruan and X. Fu (2011). Numerical simulation on fluid mixing by effects of geometry in staggered oriented ridges micromixers. *Sensors and Actuator B* 153, 284-292.

Yang, S. M., S. Lv, W. Zhang and Y. Cui (2022). Microfluidic Point-of-Care (POC) Devices in

Early Diagnosis: A Review of Opportunities and Challenges. *Sensors* 22, 1620.

Zhang, S., X. Chen, Z. Wu and Y. Zheng (2019). Numerical study on stagger Koch fractal baffles micromixer. *International Journal of Heat and Mass Transfer* 133, 1065-1073.